Hindawi
International Journal of Aerospace Engineering
Volume 2022, Article ID 1911820, 11 pages
https://doi.org/10.1155/2022/1911820

Research Article

Finite-Time Orbit Control for Spacecraft Formation with External Disturbances and Limited Data Communication

Lei Xing,[1] **Dechao Ran**,[2] **Jian Zhang**,[3] **and Li Huang**[4]

[1]*Research Center of Satellite Technology, Harbin Institute of Technology, Harbin 150001, China*
[2]*National Innovation Institute of Defense Technology, Chinese Academy of Military Science, Beijing 100000, China*
[3]*Shanghai Institute of Satellite Engineering, Shanghai 200000, China*
[4]*Beijing Aerospace Automatic Control Institute, Beijing 100000, China*

Correspondence should be addressed to Lei Xing; xinglei@hit.edu.cn

Received 25 October 2021; Revised 11 January 2022; Accepted 15 March 2022; Published 9 May 2022

Academic Editor: Angelo Cervone

This work addresses the finite-time orbit control problem for spacecraft formation flying with external disturbances and limited data communication. A hysteretic quantizer is employed for data quantization in the controller-actuator channel to decrease the communication rate and prevent the chattering phenomenon caused by the logarithmic quantizer. Combined with the adding one power integrator method and backstepping technique, a new finite-time tracking control strategy with adaptation law is designed to ensure that the closed-loop system is practical finite-time stable, and that the tracking errors of relative position and velocity are bounded within finite-time despite with limited data communication and external disturbances. Finally, an example is shown to validate the effectiveness of the proposed finite-time tracking controller.

1. Introduction

Spacecraft formation flying (SFF) is a concept that the functionality of traditional large spacecraft is replaced by a group of less-expensive, smaller, and cooperative spacecraft [1, 2]. In recent years, the study of spacecraft formation control has gradually became an active area of research owing to the reason that SFF is a primary technology for modern space missions, such as deep space exploration, spacecraft on-orbit servicing, and deep space imaging [3–6]. So far, a rich body of orbit control strategies for SFF has been presented, and the relative dynamic model of these strategies can be roughly categorized into two types, namely, linear dynamic model and nonlinear dynamic model [7, 8]. Considering the linearizing of relative dynamic model can induce model errors, various control schemes based on the nonlinear relative dynamic model for spacecraft formation flying have been proposed [9–12].

It is to be noticed that all aforementioned control schemes can only guarantee the asymptotical stability of the controlled systems. A fast convergence rate is an essential demand for SFF. In the past few years, the finite-time control method has been widely adopted to design controllers for various nonlinear systems since it can guarantee the controlled systems have better disturbance rejection property, faster convergence rate, and higher precision control performance compared with the asymptotic control [13–16]. To date, the finite-time method has been found successfully applied to handle the spacecraft control problem [17, 18]. The design approaches for finite-time control for spacecraft main include three type approaches, namely, the adding one power integrator technique, the terminal sliding mode method, and the homogeneity theorem. However, the few studies have focused on finite-time orbit control based on the adding one power integrator technique for spacecraft formation.

Despite the fact that the mentioned research results above can ensure the controlled system finite-time stability, most of the existing finite-time control strategies focused on traditional large spacecraft, in which the bandwidth of the communication channel is assumed to be not limited. However, in modern spacecraft formation control system,

data communication between different modules is usually executed by wireless networks, which means that the bandwidth of the communication channel is limited [19, 20]. Although the use of wireless networks brings many advantages, such as lighter weight, implementation, and installation with less cost, some new challenges have inevitably been induced, for example, data missing, communication time delay, and quantization effect [21–24]. It is well known that when the data of the control module is transmitted to the actuator module by limited communication networks, the quantization errors caused by signal quantization have unavoidably emerged. If the effect of quantization errors is not compensated effectively, the control performance may be degraded or even let the system unstable. Therefore, it is desirable to design a new controller considering limited data communication for network-based spacecraft formation control systems. Recently, the attitude control problem with limited data communication for spacecraft has been studied in [25]. Unfortunately, the study concentrated on finite-time control for SFF with limited data communication is scarce.

Motivated by the above discussion, the finite-time orbit control for SFF with limited data communication will be investigated. The main contribution of this work can be summarized as follows: (1) a novel finite-time tracking controller for SFF is proposed such that the tracking errors are bounded within finite time, in which the external disturbances are considered. (2) Compared with some existing finite-time controllers designed based on the terminal sliding mode method [26–28], the advantage of our method is that it can avoid noncontinuous and singular problem by using the backstepping approach and the adding one power integrator technique. (3) The needed communication rate is decreased by employing the hysteresis quantizer to quantify the control data, in which the chattering phenomenon induced by the logarithmic quantizer can be successfully prevented.

The rest of the paper is organized as follows. The modeling and preliminaries are given in Section 2. In Section 3, the main results are presented. In Section 4 and Section 5, the illustrative example and conclusions are presented, respectively.

2. Modeling and Preliminaries

2.1. Spacecraft Formation Flying Dynamic Model. The nonlinear relative motion dynamics of SFF can be described as follows [29]:

$$\begin{cases} \ddot{x} - 2n\dot{y} - \dot{n}y - n^2x = -\dfrac{\mu x}{\|R + q_1(t)\|^3} - \dfrac{u_{l1}}{m_l} + w_1 + \dfrac{u_1}{m_f}, \\ \ddot{y} + 2n\dot{x} + \dot{n}x - n^2y = \dfrac{u_2}{m_f} - \dfrac{\mu(y+r)}{\|R + q_1(t)\|^3} + \dfrac{\mu r}{\|R\|^3} - \dfrac{u_{l2}}{m_l} + w_2, \\ \ddot{z} + \dfrac{\mu z}{\|R + q_1(t)\|^3} + \dfrac{u_{l3}}{m_l} = w_3 + \dfrac{u_3}{m_f}, \end{cases} \tag{1}$$

where $q_1(t) = [x, y, z]^T$ is the relative position from the follower spacecraft to the leader spacecraft in the local coordinate frame, $u(t) = [u_1, u_2, u_3]^T$ and $u_l(t) = [u_{l1}, u_{l2}, u_{l3}]^T$ are the control inputs of the follower spacecraft and leader spacecraft, respectively, m_f and m_l denote the mass of the follower spacecraft and leader spacecraft, respectively, $w(t) = [w_1, w_2, w_3]^T$ denotes the bounded external disturbance, μ denotes the Earth gravitational constant, n denotes the orbit angular velocity of the leader spacecraft, and $R = (0, r, 0)^T$ is the position vector from the inertial coordinate attached to the center of Earth to the leader spacecraft described in the local coordinate frame.

The position tracking error $e_1(t)$ and velocity tracking error $e_2(t)$ are defined as

$$e_1(t) = q_1(t) - q_{1d} = [e_{11}, e_{12}, e_{13}]^T, \quad e_2(t) = q_2(t) - q_{2d} = [e_{21}, e_{22}, e_{23}]^T, \tag{2}$$

where $q_2(t) = [\dot{x}, \dot{y}, \dot{z}]^T$, $q_{1d} = [x_d, y_d, z_d]^T$ m, and $q_{2d} = [\dot{x}_d, \dot{y}_d, \dot{z}_d]^T$ m/s are the relative velocity vector, desired position state, and desired velocity state, respectively.

Then, the error relative motion dynamics of SFF can be described as follows:

$$\begin{cases} \dot{e}_1(t) = e_2(t), \\ \dot{e}_2(t) = f(q_1, q_2, \dot{q}_{2d}) + \dfrac{1}{m}(u(t) + w(t)) \end{cases}, \tag{3}$$

where

$$\begin{aligned} f(q_1, q_2, \dot{q}_{2d}) &= \begin{bmatrix} f_1(q_{11}, q_{21}, \dot{q}_{2d1}) \\ f_2(q_{12}, q_{22}, \dot{q}_{2d2}) \\ f_3(q_{13}, q_{23}, \dot{q}_{2d3}) \end{bmatrix} \\ &= \begin{bmatrix} 2n\dot{y} + \dot{n}y + n^2x - \dfrac{\mu x}{\|R + q_1(t)\|^3} - \dfrac{u_{l1}}{m_l} - \ddot{x}_d \\ -2n\dot{x} - \dot{n}x + n^2y - \dfrac{\mu(y+r)}{\|R + q_1(t)\|^3} + \dfrac{\mu r}{\|R\|^3} - \dfrac{u_{l2}}{m_l} - \ddot{y}_d \\ -\dfrac{\mu z}{\|R + q_1(t)\|^3} - \dfrac{u_{l3}}{m_l} - \ddot{z}_d \end{bmatrix}. \\ f(q_1, q_2, \dot{q}_{2d}) &= [f_1(q_{11}, q_{21}, \dot{q}_{2d1}), f_2(q_{12}, q_{22}, \dot{q}_{2d2}), f_3(q_{13}, q_{23}, \dot{q}_{2d3})]^T. \end{aligned} \tag{4}$$

Assumption 1. The desired states q_{1d} and q_{2d} are assumed to bounded, and their first two-order time derivatives are assumed to be bounded.

Definition 2. The solution of (3) can be regarded as finite-time bounded or practical finite-time stable if for all $e(0) = e_0$, and there exists $\bar{\nu} > 0$ and $T_r(\bar{\nu}, e_0) < \infty$, such that $\|e(t)\| < \bar{\nu}$ for $t \geq T_r$.

Lemma 3 (see [30]). *For $x_i \in R$, $i = 1, \cdots, m$ if $q > 1$, we have*

$$\left(\sum_{i=1}^{m}|x_i|\right)^q \le 2^{q-1}\sum_{i=1}^{m}|x_i|^q,$$
$$\left(\sum_{i=1}^{m}|x_i|\right)^{1/q} \le \sum_{i=1}^{m}|x_i|^{1/q}. \tag{5}$$

Lemma 4 (see [31]). *If α and β be positive constants, then $\varsigma(y, z) > 0$ is a real-valued function. We have*

$$|y|^{\alpha}|z|^{\beta} \le \frac{\alpha\varsigma(y,z)}{\alpha+\beta}|y|^{\alpha+\beta} + \frac{\beta\varsigma(y,z)^{-\alpha/\beta}}{\alpha+\beta}|z|^{\alpha+\beta}. \tag{6}$$

2.2. Fuzzy-Logic Systems. The IF-THEN rules of the FLSs are constructed:

$$R^l: \text{if } x_1 \text{ is } \mathfrak{F}_1^l, x_2 \text{ is } \mathfrak{F}_2^l, \cdots, \text{and } x_n \text{ is } \mathfrak{F}_n^l, \text{then } y \text{ is } \mathfrak{G}^l, \tag{7}$$

where $x = [x_1, \cdots, x_n]^T \in \mathbb{R}^n$ is the input of FLSs, $y \in \mathbb{R}$ is the output of FLSs, and $\mathfrak{F}_i^l$ and $\mathfrak{G}^l$ are the fuzzy sets associate with the membership functions $\mu_{\mathfrak{F}_2^l}(x_i)$ and $\mu_{\mathfrak{G}^l}(y)$, respectively. $m = 1, 2, \cdots, k$ and k are the number of rules. Then, the FLSs can be expressed as

$$y(x) = \frac{\sum_{m=1}^{k}\Lambda_m\prod_{i=1}^{n}\mu_{\mathfrak{F}_i^m}(x_i)}{\sum_{m=1}^{k}\prod_{i=1}^{n}\mu_{\mathfrak{F}_i^m}(x_i)}, \tag{8}$$

where $\Lambda_m = \max_{y\in\mathbb{R}}\mu_{\mathfrak{G}^m}(y)$, and the fuzzy basis functions can be expressed by

$$\xi_m(x) = \frac{\prod_{i=1}^{n}\mu_{\mathfrak{F}_i^m}(x_i)}{\sum_{l=1}^{k}\left[\prod_{i=1}^{n}\mu_{\mathfrak{F}_i^m}(x_i)\right]}. \tag{9}$$

Let $\Lambda^T = [\Lambda_1, \Lambda_2, \cdots, \Lambda_k]$ and $\xi^T(x) = [\xi_1, \xi_2, \cdots, \xi_k]$. Based on (9), we have $\xi^T(x)\xi(x) < 1$. Then, considering (8) and (9), we can obtain

$$y(x) = \Lambda^T\xi(x). \tag{10}$$

Moreover, we can obtain the following property when the membership function is the Gaussian function.

Lemma 5 (see [32]). *If $f(x)$ is a continuous function defined on a compact set Ω, then there exists an FLSs for any given positive constant $\varepsilon^* > 0$ satisfying*

$$\sup_{x\in\Omega}\left|f(x) - \Lambda^{*T}\xi(x)\right| \le \varepsilon^*, \tag{11}$$

where Λ^* is the optimal parameter vector.

It is well known that FLSs have been used to deal with the uncertainties of nonlinear control systems owing to their universal approximation ability. In this paper, the FLSs will be used to approximate $\Omega(\mathfrak{R}_{2i})$.

2.3. Hysteretic Quantizer. In this paper, the hysteresis quantizer $Q(\cdot)$ is introduced to quantify the control signal, which can be expressed as follows [33]:

$$Q(u_i) \triangleq \begin{cases} u_{ik}\ \mathrm{sgn}\ (u_i) & \text{if } \dfrac{u_{ik}}{1+\eta} < |u_i| \le \dfrac{u_{ik}}{1-\eta}, \dot{u}_{ik} < 0, \\ & u_{ik} < |u_i| \le \dfrac{u_{ik}}{1-\eta}, \dot{u}_{ik} > 0, \\ u_{ik}(1+\delta)\ \mathrm{sgn}\ (u_i) & \text{if } u_{ik} < |u_i| \le \dfrac{u_{ik}}{1-\eta}, \dot{u}_{ik} < 0, \\ & \dfrac{u_{ik}}{1-\eta} \le |u_i| \le \dfrac{u_{ik}(1+\eta)}{1-\eta}, \dot{u}_{ik} > 0, \\ 0, & \text{if } 0 \le |u_i| < \dfrac{u_{\min}}{1+\eta}, \dot{u}_{ik} < 0, \\ & \dfrac{u_{\min}}{1+\eta} \le |u_i| \le u_{\min}, \dot{u}_{ik} > 0, \\ Q(u_i)(t^-) & \text{othercase} \end{cases} \tag{12}$$

where

$$u_{ik} = \rho^{(1-k)}u_{\min}, \quad k = 1, 2, \cdots n, \tag{13}$$

and $u_{\min} > 0$, $0 < \rho < 1$, and $\eta = 1 - \rho/1 + \rho$. $Q(u_i)$ is in the set of $U = \{0, \pm u_{ik}, \pm u_{ik}(1+\delta)\}$. The size of the dead-zone for $Q(u_i)$ is determined by $u_{\min}$. The map of the hysteresis quantizer $Q(u_i)$ for $u_i > 0$ is given in Figure 1.

Remark 6. The parameter ρ can be considered as a measure of quantization density. From (13), it is well known that the smaller ρ is, the coarser the quantizer becomes. Furthermore, η approaches 1 while ρ approaches zero, and then $Q(u_i)$ will have fewer quantization levels since u_i ranges over that interval [34]. Thus, the needed communication rate between the actuator module and control module is lower.

Remark 7. Unlike the logarithmic quantizer, additional quantization levels have been added in (12) to prevent oscillations. Besides, the parameter ρ chosen should be based on a principle that the controlled system is stable can be ensured.

To facilitate the next controller design, the hysteretic quantizer $Q(u_i)$ is decomposed into the following form:

$$Q(u_i) = \phi_i(t)u_i + d_i(t), \tag{14}$$

where $\phi_i(t)$ and $d_i(t)$ are nonlinear functions.

Lemma 8. *The nonlinear blue functions $\phi_i(t)$ and $d_i(t)$, respectively, satisfy*

$$1 - \eta \le \phi_i(t) \le 1 + \eta, |d_i(t)| \le u_{\min}. \tag{15}$$

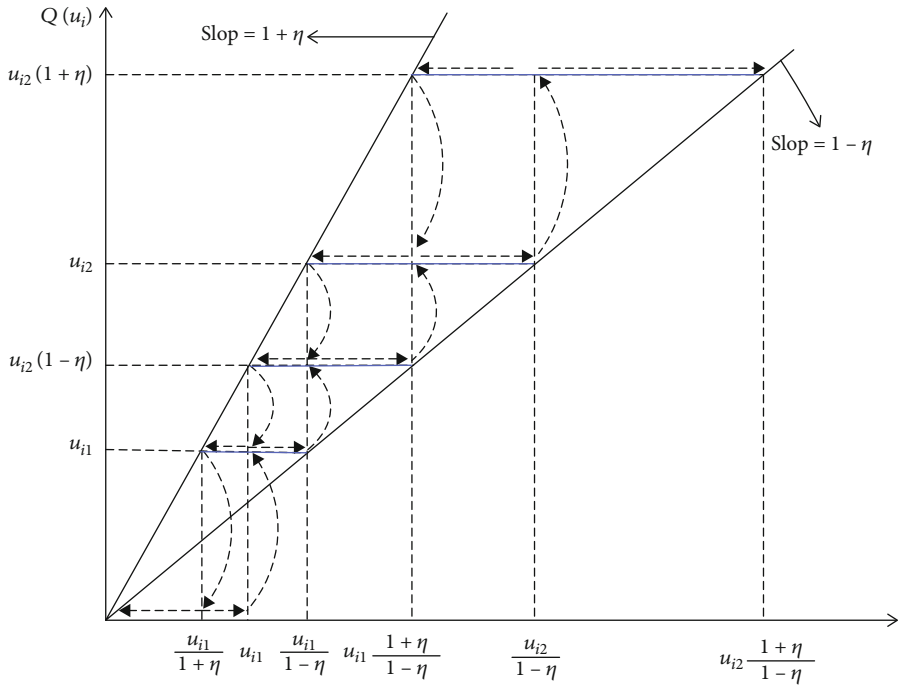

Figure 1: Map of $Q(u_i)$ for $u_i > 0$.

Proof. From Figure 2 and according to the sector-bound properties, for $|u_i| \geq u_{\min}$, we have

$$(1-\eta)u_i \leq Q(u_i) \leq (1+\eta)u_i(t). \tag{16}$$

For $|u_i| \leq u_{\min}$, when $Q(u_i) = 0$, one has

$$0 = \phi_i(t)u_i + d_i(t). \tag{17}$$

□

Define

$$\phi_i(t) = \begin{cases} \dfrac{Q(u_i)}{u_i}, & |u_i| > u_{\min} \\ 1, & |u_i| \leq u_{\min} \end{cases} \quad d_i(t) = \begin{cases} 0 & |u_i| > u_{\min} \\ -u_i(t), & |u_i| \leq u_{\min} \end{cases}. \tag{18}$$

Then, $Q(u_i) = \phi_i(t)u_i + d_i(t)$ holds, where $\phi_i(t)$ and $d_i(t)$ satisfy (15).

2.4. Control Objective. The objective of this paper is to develop a finite-time adaptive tracking controller $u(t)$ such that the position state $q_1(t)$ and velocity state $q_2(t)$ can track the desired state q_{1d} and q_{2d} in finite-time, and that the tracking error states $e_1(t)$ and $e_2(t)$ are finite-time bounded with limited data communication and external disturbances.

3. Main Results

In this section, a novel finite-time orbit tracking control strategy for formation spacecraft will be proposed. To facilitate the control strategy propose, the intermediate variables

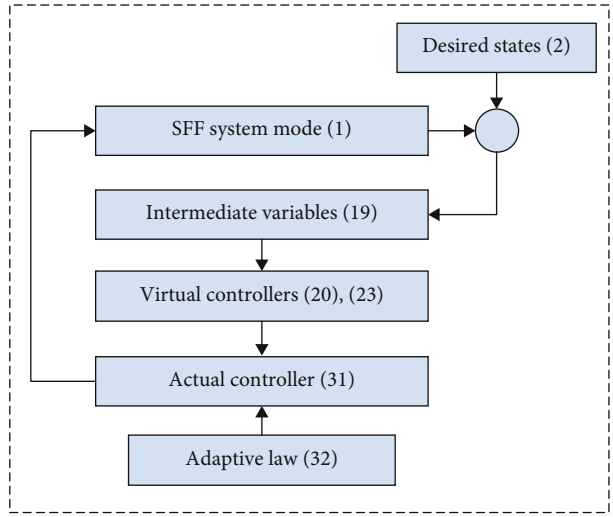

Figure 2: Block diagram of the finite-time control scheme.

$\mathfrak{R}_{1i}$ and $\mathfrak{R}_{2i}$ is defined as follows:

$$\begin{aligned} \mathfrak{R}_{1i} &= e_{1i}^{1/\alpha_1} - \sigma_{1i}^{1/\alpha_1}, \\ \mathfrak{R}_{2i} &= e_{2i}^{1/\alpha_2} - \sigma_{2i}^{1/\alpha_2}, \; i = 1, 2, 3, \end{aligned} \tag{19}$$

where $\alpha_1 = 1$, $0 < \alpha_2 = 1 + \tau < 1$, and $\tau = -m/n < 0$ be the ration of an even integer m and an odd integer n. σ_{1i} and σ_{2i} are the virtual controller. Under the backstepping method framework, the control strategy develop procedure is described as follows:

Step 1. Propose of virtual control law σ_{1i} and σ_{2i}.

Consider a Lyapunov function candidate as $V_1 = \sum_{i=1}^{3} \int_{\sigma_{1i}}^{e_{1i}} \left(s^{1/\alpha_1} - {\sigma_{1i}}^{1/\alpha_1}\right)^{2-\alpha_2} ds$.

Design the virtual controller σ_{1i} as follows:

$$\sigma_{1i} = 0. \tag{20}$$

The derivative of V_1 is obtained as follows:

$$\dot{V}_1 = \sum_{i=1}^{3} {\mathfrak{R}_{1i}}^{2-\alpha_2} \dot{e}_{1i} = \sum_{i=1}^{3} {\mathfrak{R}_{1i}}^{2-\alpha_2} (e_{2i} - \sigma_{2i}) + \sum_{i=1}^{3} {\mathfrak{R}_{1i}}^{2-\alpha_2} \sigma_{2i}, \tag{21}$$

and then applying Lemmas 3 to 5 yields

$$\begin{aligned} {\mathfrak{R}_{1i}}^{2-\alpha_2} (e_{2i} - \sigma_{2i}) &\le \left| {\mathfrak{R}_{1i}}^{2-\alpha_2} (e_{2i} - \sigma_{2i}) \right| \le 2 |\mathfrak{R}_{1i}|^{2-\alpha_2} |\mathfrak{R}_{2i}|^{\alpha_2} \\ &\le |\mathfrak{R}_{1i}|^2 + \varsigma |\mathfrak{R}_{2i}|^2, \end{aligned} \tag{22}$$

where $\varsigma = \alpha_2 (2 - \alpha_2)^{(2-\alpha_2)/\alpha_2} > 0$ is a positive constant. The virtual control scheme is proposed as

$$\sigma_{2i} = -2\mathfrak{R}_{1i}^{\alpha_2}. \tag{23}$$

Then substituting (22) and (23) into above (21)

$$\begin{aligned} \dot{V}_1 &\le \sum_{i=1}^{3} |\mathfrak{R}_{1i}|^2 + \sum_{i=1}^{3} \varsigma |\mathfrak{R}_{2i}|^2 + \sum_{i=1}^{3} \left({\mathfrak{R}_{1i}}^{2-\alpha_2} \right) \sigma_{2i} \le \sum_{i=1}^{3} |\mathfrak{R}_{1i}|^2 \\ &\quad + \sum_{i=1}^{3} \varsigma |\mathfrak{R}_{2i}|^2 - 2 \sum_{i=1}^{3} \mathfrak{R}_{1i}^2 \le \sum_{i=1}^{3} \varsigma |\mathfrak{R}_{2i}|^2 - \sum_{i=1}^{3} \mathfrak{R}_{1i}^2. \end{aligned} \tag{24}$$

Step 2. Propose of controller u_i.

Consider the Lyapunov function as follows:

$$V = V_1 + \varpi + 1/2 \sum_{i=1}^{3} \tilde{\psi}_i^2, \tag{25}$$

where $0 < \alpha_2 + \tau < 1$

$$\varpi = \sum_{i=1}^{3} \int_{\sigma_{2i}}^{e_{2i}} \left(s^{1/\alpha_2} - {\sigma_{2i}}^{1/\alpha_2} \right)^{2-\alpha_3} ds. \tag{26}$$

The time derivative of ϖ is derived as

$$\dot{\varpi} = \sum_{i=1}^{3} \mathfrak{R}_{2i}^{2-\alpha_3} \dot{e}_{2i} + \sum_{i=1}^{3} (2 - \alpha_3) \frac{-d\left({\sigma_{2i}}^{1/\alpha_2}\right)}{dt} \int_{\sigma_{2i}}^{e_{2i}} \left(s^{1/\alpha_2} - {\sigma_{2i}}^{1/\alpha_2} \right)^{1-\alpha_3} ds. \tag{27}$$

Note that

$$\int_{\sigma_{2i}}^{e_{2i}} \left(s^{1/\alpha_2} - {\sigma_{2i}}^{1/\alpha_2} \right)^{1-\alpha_3} ds \le |\mathfrak{R}_{2i}|^{1-\alpha_3} |e_{2i} - \sigma_{2i}| \le 2^{1-\alpha_2} |\mathfrak{R}_{2i}|^{1-\tau} \le 2 |\mathfrak{R}_{2i}|^{1-\tau}. \tag{28}$$

Based on (28), we have

$$\begin{aligned} &(2 - \alpha_3) \frac{-d\left({\sigma_{2i}}^{1/\alpha_2}\right)}{dt} \int_{\sigma_{2i}}^{e_{2i}} \left(s^{1/\alpha_2} - {\sigma_{2i}}^{1/\alpha_2} \right)^{1-\alpha_3} ds \\ &\quad \le (2 - \alpha_3) 2^{1+\alpha_2/\alpha_2} e_{2i} |\mathfrak{R}_{2i}|^{1-\tau} \triangleq \chi(e_{2i}, \sigma_{2i}). \end{aligned} \tag{29}$$

Substituting (29) into the time derivative of V, it yields

$$\begin{aligned} \dot{V} &= \dot{V}_1 + \dot{\varpi} + \sum_{i=1}^{3} \tilde{\psi}_i \tilde{\psi}_i \le \sum_{i=1}^{3} \varsigma |\mathfrak{R}_{2i}|^2 - \sum_{i=1}^{3} \mathfrak{R}_{1i}^2 + \sum_{i=1}^{3} \mathfrak{R}_{2i}^{2-\alpha_3} \dot{e}_{2i} \\ &\quad + \chi(e_{2i}, \sigma_{2i}) + \sum_{i=1}^{3} \tilde{\psi}_i \tilde{\psi}_i \le \sum_{i=1}^{3} \varsigma |\mathfrak{R}_{2i}|^2 - \sum_{i=1}^{3} \mathfrak{R}_{1i}^2 \\ &\quad + \sum_{i=1}^{3} \mathfrak{R}_{2i}^{2-\alpha_3} (\mathfrak{R}_{2i}) \left(f_i(q_{1i}, q_{2i}, \dot{q}_{2di}) + \frac{1}{m} (Q(u_i) + w_i) \right) \\ &\quad + \chi(e_{2i}, \sigma_{2i}) - \sum_{i=1}^{3} \tilde{\psi}_i \dot{\hat{\psi}}_i. \end{aligned} \tag{30}$$

The controller u_i is designed as

$$u_i = -\frac{m}{1 - \eta} \left(\mathfrak{R}_{2i}^{\alpha_3} \left(\ell_i \hat{\psi}_i + 1 \right) + f_i(q_{1i}, q_{2i}, \dot{q}_{2di}) \right). \tag{31}$$

The adaptive law of $\hat{\psi}_i$ is designed as

$$\dot{\hat{\psi}}_i = \ell_i \mathfrak{R}_{2i}^2 - \mu_i \hat{\psi}_i, \tag{32}$$

where $\ell_i > 0$ and $\mu_i > 0$ are designed parameters.

Substituting (31) into (30) yields

$$\begin{aligned} \dot{V} &\le \sum_{i=1}^{3} \varsigma |\mathfrak{R}_{2i}|^2 - \sum_{i=1}^{3} \mathfrak{R}_{1i}^2 + \sum_{i=1}^{3} \mathfrak{R}_{2i}^{2-\alpha_3} \\ &\quad \cdot \left(f_i(q_{1i}, q_{2i}, \dot{q}_{2di}) + \frac{1}{m} (\phi_i(t) u_i + d_i(t) + w_i) \right) \\ &\quad + \sum_{i=1}^{3} \chi(e_{2i}, \sigma_{2i}) - \sum_{i=1}^{3} \tilde{\psi}_i \dot{\hat{\psi}}_i \le \sum_{i=1}^{3} \varsigma |\mathfrak{R}_{2i}|^2 \\ &\quad - \sum_{i=1}^{3} \mathfrak{R}_{1i}^2 + \mathfrak{R}_{2i}^{2-\alpha_3} \left(\frac{1}{m} (d_i(t) + w_i) \right) - \sum_{i=1}^{3} \mathfrak{R}_{2i}^2 \left(\ell_i \hat{\psi}_i + 1 \right) \\ &\quad + \sum_{i=1}^{3} \chi(e_{2i}, \sigma_{2i}) - \sum_{i=1}^{3} \tilde{\psi}_i \dot{\hat{\psi}}_i. \end{aligned} \tag{33}$$

Let $\Omega(\mathfrak{R}_{2i}) = \mathfrak{R}_{2i}^{\tau-1}(\varsigma|\mathfrak{R}_{2i}|^2 + \mathfrak{R}_{2i}^{2-\alpha_3}((1/m)(d_i(t) + w_i)) + \chi(e_{2i}, \sigma_{2i}))$. Then, (33) can be rewritten as

$$\dot{V} \le -\sum_{i=1}^{3}\mathfrak{R}_{1i}^2 - \sum_{i=1}^{3}\mathfrak{R}_{2i}^2\left(\ell_i\widehat{\psi}_i + 1\right) - \sum_{i=1}^{3}\tilde{\psi}_i\dot{\widehat{\psi}}_i + \sum_{i=1}^{3}\mathfrak{R}_{2i}^{1-\tau}\Omega(\mathfrak{R}_{2i}). \tag{34}$$

By using the approximation ability of FLSs in Lemma 5, we have

$$\Omega(\mathfrak{R}_{2i}) = \varphi_i(\mathfrak{R}_{2i})^{*T}\xi_i + \varepsilon_1. \tag{35}$$

For convenience, let

$$\Omega = \varphi_i^{*T}\xi_i + \varepsilon_1 \le \bar{\varphi}_i^{*T}\bar{\xi}_i, \tag{36}$$

where φ_i^{*T} is the optimal fuzzy weight vector, $|\varepsilon_1| \le \varepsilon_1^*$, with ε_1^* being a positive constant. $\bar{\varphi}_i^{*T} = [\varphi_i^{*T}, \varepsilon_1^*]$ and $\bar{\xi}_i^T = [\xi_i^T, 1]$. According to Lemmas 3 to 4, and noting that $0 < \xi_i^T\xi_i \le 1$, one has

$$\mathfrak{R}_{2i}^{1-\tau}\Omega \le |\mathfrak{R}_{2i}|^{1-\tau}\psi_i^{1-\tau 2} \le \ell_i\mathfrak{R}_{2i}^2\psi_i + \Gamma_i, \tag{37}$$

where $\tilde{\psi}_i = \psi_i - \widehat{\psi}_i$, $\psi = (\sqrt{2}\|\bar{\varphi}_i^*\|)^{2/(1-\tau)}$, and $\ell_i > 0$ are positive design parameters, $\Gamma_i = (1+\tau/2)((2/1-\tau)\ell_i)^{-1-\tau/1+\tau}$, and $\widehat{\psi}_i$ is the estimate of the parameter ψ_i. Substituting (32) and (37) into (34) yields

$$\begin{aligned}\dot{V} &\le -\sum_{i=1}^{3}\mathfrak{R}_{1i}^2 - \sum_{i=1}^{3}\mathfrak{R}_{2i}^2\left(\ell_i\widehat{\psi}_i + 1\right) - \sum_{i=1}^{3}\tilde{\psi}_i\dot{\widehat{\psi}}_i + \sum_{i=1}^{3}\ell_i\mathfrak{R}_{2i}^2\psi_i \\ &+ \sum_{i=1}^{3}\Gamma_i \le -\sum_{i=1}^{3}\mathfrak{R}_{1i}^2 - \sum_{i=1}^{3}\mathfrak{R}_{2i}^2\left(\ell_i\widehat{\psi}_i + 1\right) \\ &- \sum_{i=1}^{3}\tilde{\psi}_i\left(\ell_i\mathfrak{R}_{2i}^2 - \mu_i\widehat{\psi}_i\right) + \sum_{i=1}^{3}\ell_i\mathfrak{R}_{2i}^2\psi_i + \sum_{i=1}^{3}\Gamma_i \le -\sum_{i=1}^{3}\mathfrak{R}_{1i}^2 \\ &- \sum_{i=1}^{3}\mathfrak{R}_{2i}^2 + \sum_{i=1}^{3}\mu_i\tilde{\psi}_i\widehat{\psi}_i + \sum_{i=1}^{3}\Gamma_i.\end{aligned} \tag{38}$$

The main theorem of this paper is presented as follows.

Theorem 9. *Consider the dynamic model of SFF described by (1) with the hysteretic quantizer given in (14). If the controller is designed as (31), and the adaptation law is given in (32), then the tracking errors e_{1i} and e_{2i}, $i = 1, 2, 3$ will converge into a region of the origin within finite-time.*

Proof. Denoting $\bar{V} = V_1 + \bar{\omega}$, one has

$$\bar{V} = \sum_{j=1}^{2}\sum_{i=1}^{3}\int_{\sigma_{ji}}^{e_{ji}}\left(s^{1/\alpha_j} - \sigma_{ji}^{1/\alpha_j}\right)^{2-\alpha_{j+1}}ds \le 2\sum_{i=1}^{3}|\mathfrak{R}_{1i}|^{2-\tau} + 2\sum_{i=1}^{3}|\mathfrak{R}_{2i}|^{2-\tau}. \tag{39}$$

Choosing $0 < \gamma = 2/2 - \tau < 1$, and according to Lemma 3, one then has

$$\bar{V}^{\gamma} \le \left(2\sum_{i=1}^{3}|\mathfrak{R}_{1i}|^{2-\tau} + 2\sum_{i=1}^{3}|\mathfrak{R}_{2i}|^{2-\tau}\right)^{\gamma} \le 2\sum_{i=1}^{3}\mathfrak{R}_{1i}^2 + 2\sum_{i=1}^{3}\mathfrak{R}_{2i}^2. \tag{40}$$

According to the definition of V and $\bar{V}$, we can obtain

$$V = \bar{V} + \frac{1}{2}\sum_{i=1}^{3}\tilde{\psi}_i^2 \tag{41}$$

According to (38) and (39), one has

$$\begin{aligned}\dot{V} &\le -\frac{1}{2}V^{\gamma} + \frac{1}{2}V^{\gamma} - \sum_{i=1}^{3}\mathfrak{R}_{1i}^2 - \sum_{i=1}^{3}\mathfrak{R}_{2i}^2 + \sum_{i=1}^{3}\mu_i\tilde{\psi}_i\widehat{\psi}_i + \sum_{i=1}^{3}\Gamma_i \\ &\le -\frac{1}{2}V^{\gamma} + \frac{1}{2}\bar{V}^{\gamma} + \frac{1}{2}\left(\frac{1}{2}\sum_{i=1}^{3}\tilde{\psi}_i^2\right)^{\gamma} - \sum_{i=1}^{3}\mathfrak{R}_{1i}^2 - \sum_{i=1}^{3}\mathfrak{R}_{2i}^2 \\ &+ \sum_{i=1}^{3}\mu_i\tilde{\psi}_i\widehat{\psi}_i + \sum_{i=1}^{3}\Gamma_i \le -\frac{1}{2}V^{\gamma} + \left(\frac{1}{2}\sum_{i=1}^{3}\tilde{\psi}_i^2\right)^{\gamma} \\ &+ \sum_{i=1}^{3}\mu_i\tilde{\psi}_i\widehat{\psi}_i + \sum_{i=1}^{3}\Gamma_i.\end{aligned} \tag{42}$$

Moreover, applying Lemma 4

$$\begin{aligned}\mu_i\tilde{\psi}_i\widehat{\psi}_i &\le -\mu_i 2\tilde{\psi}_i^2 + \mu_i 2\psi_i^2, \\ \left(\frac{1}{2}\sum_{i=1}^{3}\tilde{\psi}_i^2\right)^{\gamma} &\le \sum_{i=1}^{3}\frac{\mu_i}{2}\tilde{\psi}_i^2 + \sum_{i=1}^{3}\nu_i,\end{aligned} \tag{43}$$

where $\nu_i = (1-\gamma)(\gamma/\mu_i)^{\gamma/(1-\gamma)}$. □

Then,

$$\begin{aligned}\dot{V} &\le -\frac{1}{2}V^{\gamma} + \sum_{i=1}^{3}\nu_i + \frac{\mu_i}{2}\psi_i^2 + \sum_{i=1}^{3}\Gamma_i \le -\frac{1}{2}\kappa V^{\gamma} - \frac{1}{2}(1-\kappa)V^{\gamma} \\ &+ \sum_{i=1}^{3}\nu_i + \frac{\mu_i}{2}\psi_i^2 + \sum_{i=1}^{3}\Gamma_i \le -\frac{1}{2}\kappa V^{\gamma} - \frac{1}{2}(1-\kappa)V^{\gamma} + \vartheta,\end{aligned} \tag{44}$$

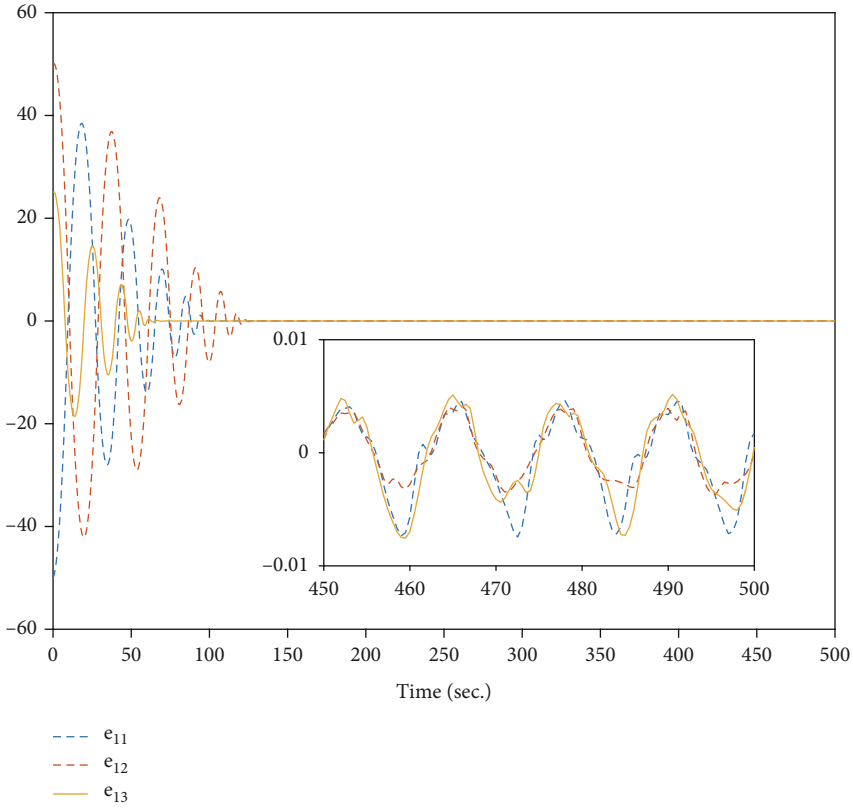

Figure 3: Response curves of position tracking errors.

where $\vartheta = \sum_{i=1}^{3} \nu_i + (\mu_i/2)\psi_i^2 + \sum_{i=1}^{3} \Gamma_i$. From (44), we can obtain that $\dot{V} \leq -12\kappa V^{\gamma}$ if and only if $V^{\gamma} > 2\vartheta/1-\kappa$, which means $V < 0$ out the set $\{V^{\gamma} \leq 2\vartheta/1-\kappa\}$. The required time of reach the bounded set is $T_r \leq 2V^{1-\gamma}(e_0)/\kappa(1-\gamma)$. Thus, as the analysis in [16], we can conclude that V can reach the set within finite time based on Definition 2. Furthermore, we can obtain that the tracking errors e_{1i} and e_{2i}, $i = 1, 2, 3$ converge into a region of the origin with finite-time.

The design procedure of the controller could be visualized from the bloc diagram shown in Figure 2.

Remark 10. By employing the property $0 < \xi_i^T \xi_i \leq 1$ of FLSs [16], only one adaptation law for $\hat{\psi}_i$ is designed to proposed the controller. Furthermore, the effects of quantization errors and external disturbances can be eliminated by the designed adaptation law.

Remark 11. Compared with the finite-time controllers using the terminal sliding mode method, the finite-time controller (31) is proposed by using the adding one power integrator technique and backstepping approach to guarantee the finite-time convergence and overcome the noncontinuous and singular problem.

4. Illustrative Example

In this section, an illustrative example is shown to illustrate the efficiency of the proposed finite-time control scheme. The leader spacecraft and follower spacecraft mass are $m_l = 1$ kg and $m_f = 1$ kg, respectively. For simplicity, the leader spacecraft is assumed in a circular reference orbit of radius 6728 km. The input control force is limited as $u_i \leq u_{\max} = 1$ N, $i = 1, 2, 3$.

The initial relative position and velocity are $q_{10} = [250, -50, 0]^T$ m and $q_{20} = [0, 0, 0]^T$ m/s, respectively. The desired relative position and relative are $q_{1d} = [0, 0, 0]^T$ m and $q_{2d} = [0, 0, 0]^T$ m/s, respectively. The external disturbance is $w(t) = [0.01 \cos(0.5t), 0.01 \cos(0.5t), 0.01 \cos(0.5t)]$. The parameters of the finite time control scheme (31) and the adaptation law (33) are chosen as $\ell_i = 0.001$, $\mu_i = 0.001$, $\hat{\psi}_i(0) = 0.01$, $i = 1, 2, 3\alpha_1 = 1$, $\alpha_2 = 3/5$, and $\alpha_3 = 1/5$, and the quantization parameters are designed as $\rho = 0.4$, $u_{\min} = 0.000001$.

The tracking errors e_{1i} and e_{2i}, $(i = 1, 2, 3)$ of the finite-time controller (31) are shown Figures 3 and 4, respectively. As observed from Figure 2, the position tracking errors can converge to almost zero with 150 s, and the position tracking errors is within $|e_{1i}| < 0.01$ m at 500 s. The control force is given in Figure 5, which force magnitude is limited to 1 N. Figure 6 shows the quantized control force for the finite-time controller (31). The response curves of $\hat{\psi}_i$ are shown in Figure 7. Clearly, the simulation results verify the validity of the hysteresis quantizer and illustrate the efficiency of the proposed finite-time control scheme.

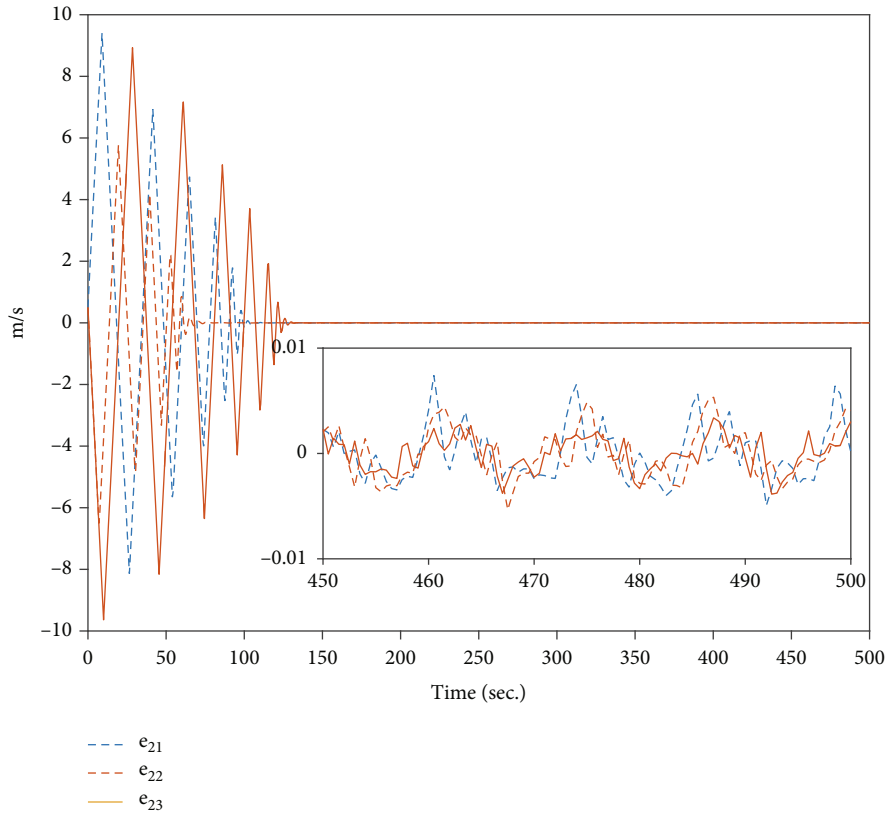

Figure 4: Response curves of velocity tracking errors.

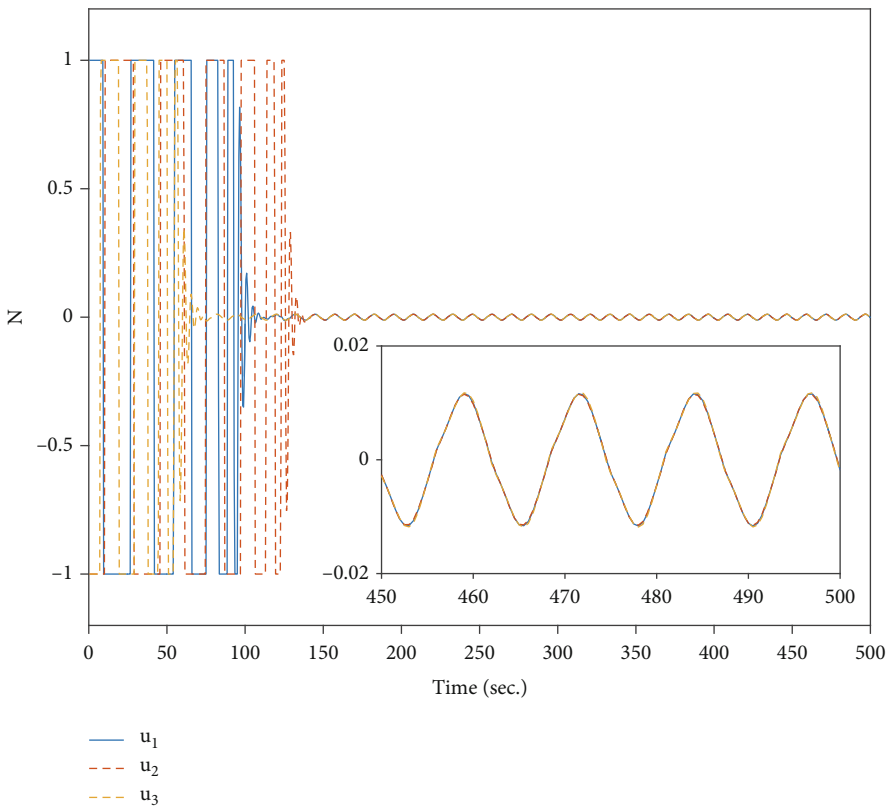

Figure 5: Response curves of control force.

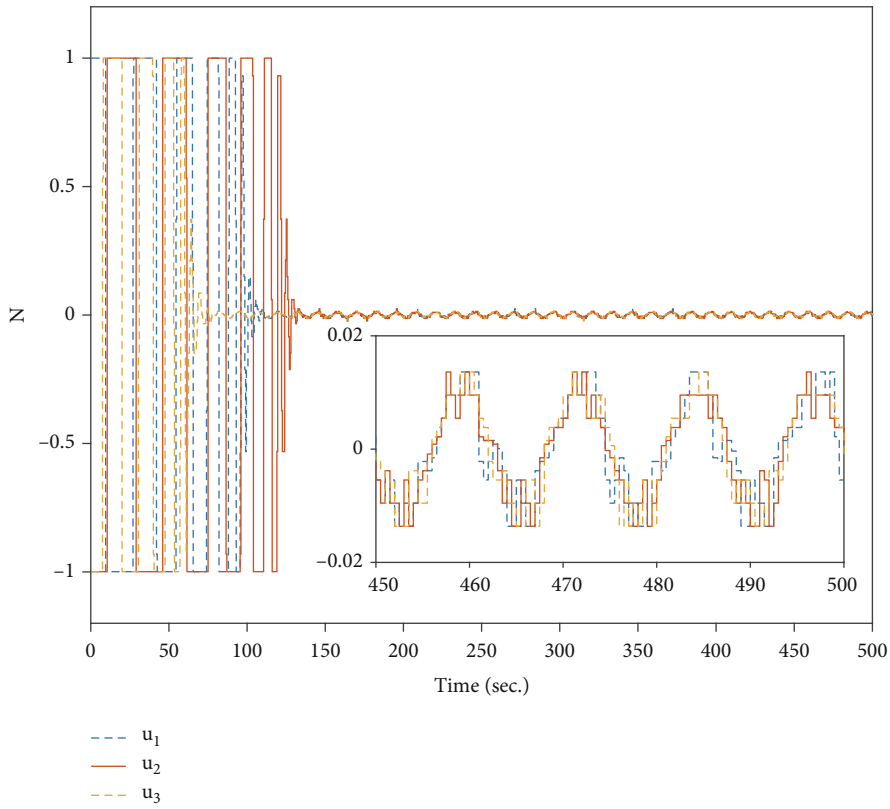

Figure 6: Response curves of quantized control force.

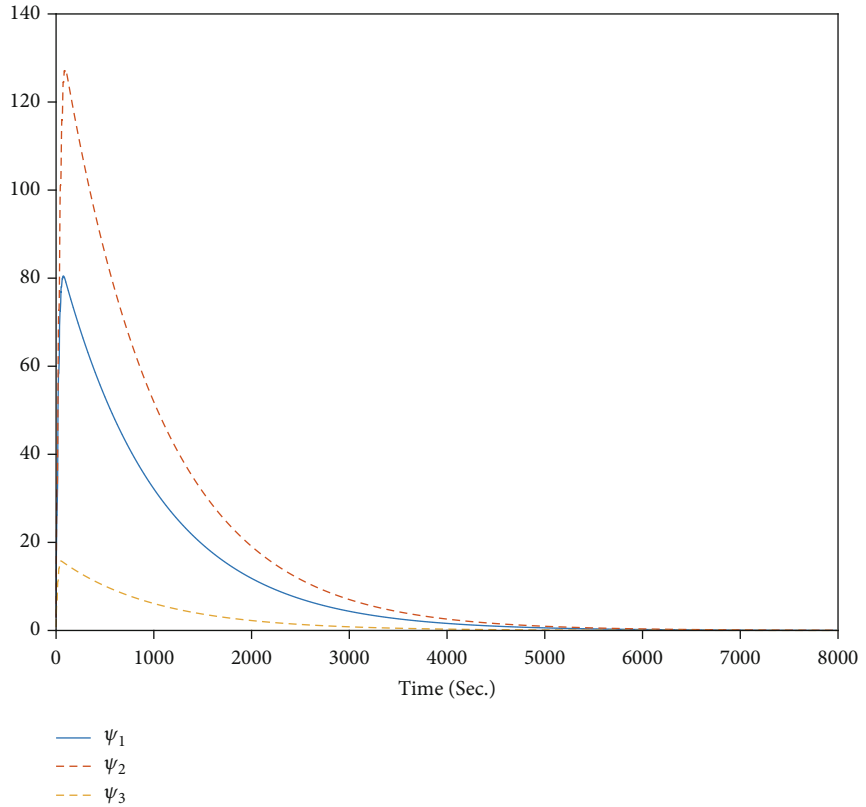

Figure 7: Response curves of the adaptive parameter $\widehat{\psi}_i$, $i = 1, 2, 3$.

5. Conclusion

In this paper, the problem of finite-time orbit control for SFF with limited data communication and external disturbances was studied. We have applied the hysteretic quantizer to quantize the data of the controller-actuator channel to decrease the communication rate. By combining with the adding one power integrator method and the backstepping technique, a finite-time adaptive controller has been developed. Under the proposed control strategy, the effects of quantization errors and external disturbances have been eliminated. Moreover, the finite-time stability of the controlled system and bounded of tracking errors of position and velocity within finite time are guaranteed by the developed controller. Finally, an example has been shown to illustrate the effectiveness of the proposed control strategy. Future work will focus on dealing with the finite-time tracking control problem for SFF with actuator faults.

Data Availability

The data used to support the findings of this study are included within the article.

Conflicts of Interest

The authors declare that they have no conflicts of interest.

References

[1] Y. Xiao, A. De Ruiter, D. Ye, and Z. Sun, "Adaptive fault-tolerant attitude tracking control for flexible spacecraft with guaranteed performance bounds," *IEEE Transactions on Aerospace and Electronic Systems*, p. 1, 2021.

[2] D. Ye, A. Zou, and Z. Sun, "Predefined-time predefined-bounded attitude tracking control for rigid spacecraft," *IEEE Transactions on Aerospace and Electronic Systems*, 2021.

[3] X. Cao, P. Shi, Z. Li, and M. Liu, "Neural-network-based adaptive backstepping control with application to spacecraft attitude regulation," *IEEE Transactions on Neural Networks and Learning Systems*, vol. 29, no. 9, pp. 4303–4313, 2018.

[4] S. M. Esmaeilzadeh, M. Golestani, and S. Mobayen, "Chattering-free fault-tolerant attitude control with fast fixed-time convergence for flexible spacecraft," *International Journal of Control, Automation and Systems*, vol. 19, no. 2, pp. 767–776, 2021.

[5] D. Lee, A. K. Sanyal, and E. A. Butcher, "Asymptotic tracking control for spacecraft formation flying with decentralized collision avoidance," *Journal of Guidance Control and Dynamics*, vol. 38, no. 4, pp. 587–600, 2015.

[6] Q. Ni, Y. Huang, and X. Chen, "Nonlinear control of spacecraft formation flying with disturbance rejection and collision avoidance," *Chinese Physics B*, vol. 26, no. 1, article 014502, 2017.

[7] L. Hui and J. Li, "Terminal sliding mode control for spacecraft formation flying," *IEEE Transactions on Aerospace and Electronic Systems*, vol. 45, no. 3, pp. 835–846, 2009.

[8] A. Zou and K. D. Kumar, "Distributed attitude coordination control for spacecraft formation flying," *IEEE Transactions on Aerospace and Electronic Systems*, vol. 48, no. 2, pp. 1329–1346, 2012.

[9] M. Chen, P. Shi, and C. Lim, "Adaptive neural fault-tolerant control of a 3-DOF model helicopter system," *IEEE Transactions on Systems, Man, and Cybernetics: Systems*, vol. 46, no. 2, pp. 260–270, 2016.

[10] Y. Lv, Q. Hu, G. Ma, and J. Zhou, "6 DOF synchronized control for spacecraft formation flying with input constraint and parameter uncertainties," *ISA Transactions*, vol. 50, no. 4, pp. 573–580, 2011.

[11] J. Shan, "Six-degree-of-freedom synchronised adaptive learning control for spacecraft formation flying," *IET Control Theory & Applications*, vol. 2, no. 10, pp. 930–949, 2008.

[12] B. Shasti, A. Alasty, and N. Assadian, "Robust distributed control of spacecraft formation flying with adaptive network topology," *Acta Astronautica*, vol. 136, pp. 281–296, 2017.

[13] E. Arabi, T. Yucelen, and J. R. Singler, "Finite-time distributed control with time transformation," *International Journal of Robust and Nonlinear Control*, vol. 31, no. 1, pp. 107–130, 2021.

[14] O. Mofid, M. Momeni, S. Mobayen, and A. Fekih, "A disturbance-observer-based sliding mode control for the robust synchronization of uncertain delayed chaotic systems: application to data security," *IEEE Access*, vol. 9, pp. 16546–16555, 2021.

[15] B. Vaseghi, S. Mobayen, S. S. Hashemi, and A. Fekih, "Fast reaching finite time synchronization approach for chaotic systems with application in medical image encryption," *IEEE Access*, vol. 9, pp. 25911–25925, 2021.

[16] A. Wang, L. Liu, J. Qiu, and G. Feng, "Finite-time adaptive fuzzy control for nonstrict-feedback nonlinear systems via an event-triggered strategy," *IEEE Transactions on Fuzzy Systems*, vol. 28, no. 9, pp. 2164–2174, 2020.

[17] D. Ran, X. Chen, and A. K. Misra, "Finite time coordinated formation control for spacecraft formation flying under directed communication topology," *Acta Astronautica*, vol. 136, pp. 125–136, 2017.

[18] A. Zou and K. Kumar, "Adaptive output feedback control of spacecraft formation flying using Chebyshev neural networks," *Journal of Aerospace Engineering*, vol. 24, no. 3, pp. 361–372, 2011.

[19] A. Bagheri, A. Jabbari, and S. Mobayen, "An intelligent ABC-based terminal sliding mode controller for load-frequency control of islanded micro-grids," *Sustainable Cities and Society*, vol. 64, article 102544, 2021.

[20] H. R. Karimi, Y. Niu, J. M. Rossell, and F. Yang, "Analysis and synthesis of control systems over wireless digital channels," *Journal of the Franklin Institute*, vol. 1, pp. 1–4, 2017.

[21] H. R. Karimi, "Robust H-infinity filter design for uncertain linear systems over network with network-induced delays and output quantization," *Modeling, Identification and Control*, vol. 30, no. 1, pp. 27–37, 2009.

[22] H. R. Karimi, M. Zapateiro, and N. Luo, "Stability analysis and control synthesis of neutral systems with time-varying delays and nonlinear uncertainties," *Chaos, Solitons & Fractals*, vol. 42, no. 1, pp. 595–603, 2009.

[23] P. Shi, Y. Zhang, M. Chadli, and R. Agarwal, "Mixed *H-Infinity* and passive filtering for discrete fuzzy neural networks with stochastic jumps and time delays," *IEEE transactions on neural networks and learning systems*, vol. 27, no. 4, pp. 903–909, 2016.

[24] D. Wang, J. Wang, and W. Wang, "Output feedback control of networked control systems with packet dropouts in both channels," *Information Sciences*, vol. 221, pp. 544–554, 2013.

[25] B. Wu, "Spacecraft attitude control with input quantization," *Journal of Guidance, Control, and Dynamics*, vol. 39, no. 1, pp. 176–181, 2016.

[26] K. Eliker and W. Zhang, "Finite-time adaptive integral backstepping fast terminal sliding mode control application on quadrotor UAV," *International Journal of Control, Automation and Systems*, vol. 18, no. 2, pp. 415–430, 2020.

[27] N. Kumar, "Finite time control scheme for robot manipulators using fast terminal sliding mode control and RBFNN," *International Journal of Dynamics and Control*, vol. 7, no. 2, pp. 758–766, 2019.

[28] G. Xia, Y. Zhang, W. Zhang, X. Chen, and H. Yang, "Dual closed-loop robust adaptive fast integral terminal sliding mode formation finite-time control for multi-underactuated AUV system in three dimensional space," *Ocean Engineering*, vol. 233, p. 108903, 2021.

[29] H. Wong, H. Pan, M. S. De Queiroz, and V. Kapila, "Adaptive learning control for spacecraft formation flying," in *Proceedings of the 40th IEEE Conference on Decision and Control (Cat. No.01CH37228),*, pp. 1089–1094, Orlando, FL, USA, 2001.

[30] Y. Li, K. Li, and S. Tong, "Adaptive neural network finite-time control for multi-input and multi-output nonlinear systems with positive powers of odd rational numbers," *IEEE transactions on neural networks and learning systems*, vol. 31, no. 7, pp. 2532–2543, 2020.

[31] C. Qian and W. Lin, "Non-Lipschitz continuous stabilizers for nonlinear systems with uncontrollable unstable linearization," *Systems & Control Letters*, vol. 42, no. 3, pp. 185–200, 2001.

[32] C. Deng and G. Yang, "Distributed adaptive fuzzy control for nonlinear multiagent systems under directed graphs," *IEEE Transactions on Fuzzy Systems*, vol. 26, no. 3, pp. 1–1366, 2017.

[33] F. Wang, Z. Liu, Y. Zhang, and C. Chen, "Adaptive quantized controller design via backstepping and stochastic small-gain approach," *IEEE Transactions on Fuzzy Systems*, vol. 24, no. 2, pp. 330–343, 2016.

[34] J. Zhou and W. Wang, "Adaptive control of quantized uncertain nonlinear systems," *IFAC-PapersOnLine*, vol. 50, no. 1, pp. 10425–10430, 2017.